Self-Sustainability in Nano Unmanned Aerial Vehicles: A Blimp Case Study

Daniele Palossi[1], Andres Gomez[1], Stefan Draskovic[1], Kevin Keller[1], Luca Benini[1,2], Lothar Thiele[1]
[2]DEI, University of Bologna, Italy. Email: luca.benini@unibo.it
[1]D-ITET, ETH Zürich, Switzerland. Email: {firstname.lastname}@ee.ethz.ch

ABSTRACT

Nowadays nano Unmanned Aerial Vehicles (UAV's), such as quadcopters, have very limited flight times, tens of minutes at most. The main constraints are energy density of the batteries and the engine power required for flight. In this work, we present a nano-sized blimp platform, consisting of a helium balloon and a rotorcraft. Thanks to the lift provided by helium, the blimp requires relatively little energy to remain at a stable altitude. We also introduce the concept of duty-cycling high power actuators, to reduce the energy requirements for hovering even further. With the addition of a solar panel, it is even feasible to sustain tens or hundreds of flight hours in modest lighting conditions (including indoor usage). A functioning 52 gram prototype was thoroughly characterized and its lifetime was measured in different harvesting conditions. Both our system model and the experimental results indicate our proposed platform requires less than 200 mW to hover in a self sustainable fashion. This represents, to the best of our knowledge, the first nano-size UAV for long term hovering with low power requirements.

CCS CONCEPTS

• **Computer systems organization → Embedded systems**;

KEYWORDS

Self sustainability, energy neutrality, UAV, blimp

ACM Reference format:
Daniele Palossi[1], Andres Gomez[1], Stefan Draskovic[1], Kevin Keller[1], Luca Benini[1,2], Lothar Thiele[1]. 2017. Self-Sustainability in Nano Unmanned Aerial Vehicles: A Blimp Case Study. In *Proceedings of CF'17, Siena, Italy, May 15-17, 2017,* 10 pages.
DOI: http://dx.doi.org/10.1145/3075564.3075580

1 INTRODUCTION

The popularity of nano unmanned aerial vehicles (nano-size UAV) in the past few years has increased dramatically. These nano-size UAVs are used for aerial mapping, photography, surveillance, sport, entertainment and many other uses. Despite significant research effort in past years, nano-size UAVs are still limited, in most cases, to tens of minutes of flight. This has limited their applicability, since longer missions require additional infrastructure to replenish them at service stations [1, 2].

CF'17, Siena, Italy

DOI: http://dx.doi.org/10.1145/3075564.3075580

A nano-sized UAV with long flight times could have a number of innovative applications in surveillance, smart buildings, agriculture and many other fields. Even if a nano-size UAV is able to fly only a few days, which is already significantly longer than existing systems, it would also be able to collect, process and transmit information from different sensors such as environmental data, audio, video and still cover a large area. Depending on the weather conditions, it could also be used in outdoor scenarios for surveillance, search and rescue, or mapping, to name a few applications.

The reduced flight times of existing UAV's are mostly due to the power required for the rotors to generate enough thrust. Even for the nano-size class of UAV's, which typically weigh ~50 g or less, around 5 W of power are needed for the mechanical system alone [3]. This does not even account for computational requirements of current research trends towards autonomous systems, which require power hungry sensor fusion and real-time control for online path planning and collision detection/avoidance algorithms [4]. Given the current battery densities of 500 J/g and their limited technology scaling, nano UAV's with flight times of days or weeks will require novel methodologies that combine both hardware and software.

Energy harvesting has been successfully demonstrated in a number of UAV platforms as a way to extend their flight times [5, 6]. Photovoltaic is a common form of harvesting due to the abundance of light and the high power density of solar cells [7]. Harvesting energy is one side of the equation, and to really maximize the lifetime of a UAV, its power requirements must be minimized as well. For many years, power management techniques like duty-cycling have been successfully deployed in battery-based cyber-physical systems in order to reduce the average power consumption and consequently extend the battery lifetime. Traditional nano UAV's, however, are fundamentally incompatible with duty-cycling. If a quadrotor tried to shut down its rotors, it will either crash very quickly or incur a significant energy penalty to counteract the acceleration due to gravity.

Fortunately, another type of UAV has certain properties which make it compatible with duty-cycling. A nano-sized blimp is a perfect candidate for long flight times because helium, a lighter-than-air gas, can provide lift and significantly reduce the energy requirements for flight. Even though helium provides lift, a perfect balance with a blimp's weight is almost impossible since even the smallest difference between the system's weight and its lift will result in an acceleration that will eventually drive the blimp to the ground, to the roof or to the stratosphere [8]. Designing a blimp that is able to hover (i.e. that is able to maintain a desired altitude within a given tolerance range) for a prolonged period of time remains a challenge to this day. Though hovering is a one dimensional problem, it is a fundamental building block for the development of fully autonomous UAVs with extended flight times.

In this work, we will explore how traditional power management techniques, usually applied to digital systems, can be extended to high power actuators, such as rotors. We demonstrate that these techniques can significantly reduce the energy requirement for hovering. We will study two types of hovering, one in which thrust is generated constantly, and another with duty-cycled rotors. The former can achieve hovering with a relatively small deviation from the desired altitude, at the price of high power consumption. The latter reduces the average power consumption and leads to a longer flight time, but introduces a larger tolerance to the desired altitude. Our proposed platform, consisting of a single rotor controlled by a low-power MCU and a $0.4\,m^3$ helium balloon, weighs a total of 52 g and is able to hover for tens to hundreds of hours, requiring only commercial-off-the-shelf components and modest light conditions. Our initial prototype has some limitations in its capability to adapt to changing environmental conditions: there is no dynamic control loop for variations in temperature, humidity and pressure. Nevertheless, it lays the ground work for an energy autonomous nano-blimp, capable of complex cognitive skills (e.g. autonomous navigation, path planning, etc.) relying only on local sensing and processing (i.e. inertial and visual), due to the relaxed real-time constraints.

The main contributions of our work are:

- A system model capable of predicting an energy harvesting blimp's lifetime given probabilistic harvesting conditions, solar panel size, and battery capacity.
- An optimization formulation for distributing a blimp's payload, thus determining the battery to solar panel weight ratio which maximizes the blimps lifetime.
- A study of two types of hovering mechanisms: constant and duty-cycling, exhibiting a trade-off between energy requirements and hovering precision.
- A thorough evaluation and model comparison of our 52 g blimp prototype. Thanks to its power management, it requires only $198\,mW$ of input power for self-sustainable hovering as opposed to $576\,mW$ needed for continuous operation of the rotor.

The remainder of this paper is organized as follows: In the next section, we discuss a general classification of UAV's with different sizes and aerodynamics, as well as existing solutions that integrate energy harvesting. In Sec. 3, we discuss the preliminary overview of hovering, and duty-cycling and self-sustainability is presented. In Sec. 4, we present our system model with probabilistic energy harvesting, and lifetime estimation. In Sec. 5, we discuss in detail the implementation of our nano-blimp prototype. In Sec. 6, we characterize our prototype and evaluate hovering with and without power management. Finally, we conclude our work in Sec. 7.

2 RELATED WORK

Unmanned Aerial Vehicles (UAVs) with solar energy harvesting, have been studied for many years. UAV's, however, can be classified according to different criteria. Each UAV class has its own challenges and limitations, which are tied to the existing technologies in the fields of mechanical propulsion, material science, and electrical engineering.

2.1 UAV Classification

Rotorcrafts can be classified on the basis of their sizes and power consumption, as reported in Tab. 1. For the sake of generality, the size refers to the core frame of the vehicle and not the inflatable parts, like balloons in the case of blimps. An additional classification parameter is the vehicle's sensitivity to environmental conditions (e.g. wind, temperature, pressure, etc.), which depends on the vehicle's dimension and speed range. The blimp presented in this paper is considered a nano UAV due to its low power consumption of ~200 mW, limited payload of 55 g, and small frame measuring about $4 \times 4\,cm$.

Vehicle Class	⊘ : Weight $[cm{:}kg]$	Power $[W]$	On-board Device
std-size[9]	$\sim 50 : \geq 1$	≥ 100	Desktop
micro-size[10]	$\sim 25 : \sim 0.5$	~ 50	Embedded
nano-size[3]	$\sim 10 : \sim 0.05$	~ 5	MCU
pico-size[11]	$\sim 2 : \sim 0.005$	~ 0.1	ULP

Table 1: Rotorcraft UAV's classification by vehicle class-size.

A second dimension for classification is the type of unmanned aerial vehicles: fixed wing, rotorcraft, and blimps. The main trade-offs between the aforementioned types are their maneuverability/controllability and their energy requirements. As depicted in Fig. 1-A, a traditional criterion to classify UAV's is given by the trade-off between *maneuverability* and *endurance* [12]. In this work we use the concept of *agility*, as shown in Fig. 1-B, defined as: the minimum space required by the vehicle to accomplish a given maneuver, at the minimum control speed. Under such definition blimps are more agile than fixed wing vehicles, since they can perform sharp turns within a limited space at reduced speeds. This notion of agility is particularly relevant for indoor applications, where human safety is an important factor. In contrast, blimps are more sensitive to environmental conditions than other UAV types, especially in outdoor scenarios.

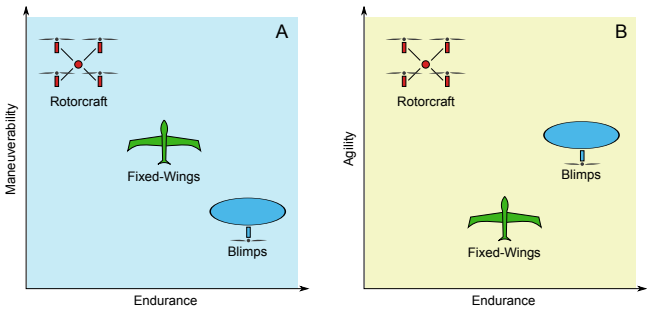

Figure 1: Classification of UAV's based on their endurance vs. maneuverability (A) and endurance vs. agility (B).

Rotorcraft These vehicles have one or more rotors and can achieve stable hovering and precise flight by adjusting rotor speed and balancing different forces. Rotorcrafts are highly maneuverable, can operate in a wide speed range and can take-off and land vertically. They also have very high energy consumption since they need to generate propulsion continuously. The most common rotorcraft is the quadrotor, that has four rotors and changes the rotation ratio among them to generate lift [10].

Fixed Wing These aircrafts, also called airplanes, use fixed wings to generate enough lift for flight. The shape of the wing pushes air over the top of the wing to flow more rapidly than underneath it, causing a difference in pressure and generating lift [13]. Though fixed-wing UAV's have lower energy requirements and longer flight times compared to quadrotors, they cannot hover or make tight turns, which can limit their deployment in certain applications. In recent years, a new hybrid category has received particular attention: *convertibles UAV's* [14]. They combine rotorcraft for take-off and landing maneuvers with fixed wing for energy-efficient long-range flights.

Blimps These vehicles, also called airships, have close to neutral buoyancy and can be steered and propelled through the air using one or more propellers [15]. Contrary to other types of UAV's, they can hover thanks to the lift generated by a lighter-than-air gas, and thus require relatively little energy for movement at low speeds. Due to their reduced energy requirements, level of *agility* and sensitivity to the environment, nano-size blimps are very suitable candidates for indoor application scenarios.

2.2 Energy Harvesting UAV's

Despite the challenges associated with high power consumption in quadrotors, researchers have been able to design solar-powered versions. The *solarcopter*, proposed in [16], uses a 0.96 m^2 monocrystalline solar panel, generating 136.8 W in favorable lighting conditions. A specially designed frame with a high stress resistance to weight ratio was required for the 925 g quadrotor to fly. Due to its lack of energy storage, this design has flight times limited to periods of high energy availability. One alternative energy source for UAV's with the potential for ultra long lifetimes are laser power beams [17]. By using a special laser power supply, a ground station can wirelessly direct power to a moving UAV. The authors of [6] present a 1 kg quadcopter prototype that was able to fly for 12.45 hours powered by laser beams. This class of systems requires line-of-sight and additional expensive infrastructure which is not feasible in many applications scenarios.

Fixed-wing UAVs have also been equipped with solar panels to harvest energy during the day. In [18], for example, the SkySailor airplane was able to fly 27 hours during summertime with a wingspan of 3.2 m using solar panels. Sunsailor [19] achieved a three day flight using a 4.2 m wingspan and weighing 3.6 kg. The Helios prototype [20] was developed by NASA for high altitude and long endurance flights. With a 75 m wingspan and a gross weight of up to 930 kg, it was able to prove sustainable in the stratosphere [5]. AtlantikSolar [13] is a 5.6m-wingspan, 6.8 kg of weight, solar-powered low-altitude long-endurance UAV capable of a continuous flight of 81.5 hours, covering a total of 2316 km. These works demonstrate that standard (and large) size fixed wing airplanes are able to harvest enough energy for long flight times. Nonetheless, it is also understood that these systems must have a scale large enough for the required energy storage systems and propulsion. In addition, these systems suffer from the same limitations of all airplanes: the inability to hover and perform sharp turns due to the minimum high speed required to operate.

Solar-powered blimps offer the best-case scenario for UAV's requiring ultra long flight times, due to their reduced energy requirements. In [21] the trade-offs between solar panel weight and power produced is chosen for a high altitude blimp and validated using design parameters from [22, 23]. In [24], the effect of the curvature of the balloon surface and the corresponding changes in the energy output is analyzed for a solar powered lighter-than-air UAV platform. All of these studies focus on large scale blimps, since they are required to withstand adverse weather conditions for prolonged periods of time, particularly those meant to operate in the stratosphere. These blimps are up to 400 m in length, and consume 100 kW. In the case of [24], the blimp has a volume of 24 m^3 and requires only 100 W of power.

Our work focuses on a nano-scale blimp that, with a weight of less than 55 g and a balloon of 0.4 m^3 can reach self-sustainability with only 198 mW of input power. To the best of our knowledge, this work presents the first nano-size UAV capable of continuous, long term hovering. Thanks to its energy harvesting capability and the low deflation rates of mylar balloons, the blimp platform presented in this paper could conceivably hover for several weeks in indoor environments.

3 PRELIMINARIES

Though there is a current trend towards autonomous and intelligent aerial vehicles, most of them are either very large systems, or have reduced flight times in the order of minutes. To understand the basic problem of why self-sustainable nano-UAV's have generally been infeasible, it is enough to look at the problem of hovering. Though it is simpler than free movement in $\mathbb{R}^3$, since it only involves translation in the vertical axis, it demonstrates the large energy requirements for nano-UAV flight.

3.1 Hovering

One of the most basic tasks that non-airplane UAV's need to perform is hovering, which keeps the aircraft at a stable altitude. Fig. 2 shows a basic comparison between a hovering quadcoptor and blimp. The quadcoptor needs to continuously generate thrust from its four rotors to be able to counteract gravity. This results in an enormous power requirement. A blimp, on the contrary, leverages a lighter-than-air gas like helium to generate lift passively. This significantly reduces the energy requirements since relatively little thrust is necessary to counteract gravity.

Though in theory a blimp can passively hover with neutral buoyancy, this is very hard to achieve in practice. For starters, choosing a passive hovering altitude would require perfectly calibrated weights to offset a balloon's lift in a given environment. Furthermore, any small change to the environmental conditions (e.g. temperature, pressure, humidity, etc.) will affect the balloon and its steady-state altitude. But even in a controlled environment, the balloon's deflation rate will quickly result in slightly negative buoyancy, which will eventually drive the balloon to the ground. For a balloon to hover long term at a desired altitude, active control is thus required. The focus of this paper is to reduce the power requirements of hovering in controlled environments to maximize the balloon's lifetime. Though a more realistic scenario includes environments with dynamic conditions, this would require adaptive control methods that simply adjust some parameters based on sensor readings (e.g. pressure sensor).

Our proposed blimp platform will be slightly a heavier-than-air system, such that it falls slowly and requires relatively little energy

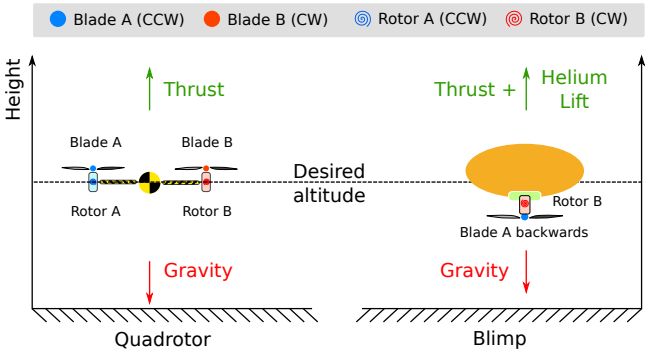

Figure 2: For a quadcopter to hover, active thrust is necessary to compensate the weight. A blimp requires significantly less thrust due to the lift generated by helium.

to achieve, on average, neutral buoyancy.[1] We want to go even further by borrowing power management concepts commonly found in digital systems and implementing them in a nano blimp. Duty-cycling is a technique in which a system periodically transitions from a power-hungry *on* state to a low power *off* state. Depending on the ratio between *on* and *off* times, the average performance and power consumption of the system will vary. The main factors that determine the total energy savings are the power consumption in the *off* state and the transition costs between *on* and *off*, since duty-cycling incurs this overhead in each cycle.

Fig. 3 shows two hovering methods for blimps in controlled environments. On the left, a constantly powered low-intensity rotor can maintain a stable altitude. On the right, duty-cycling a high-intensity rotor can achieve, on average, the desired altitude. It might seem counter-intuitive that even though duty-cycling requires a higher rotor intensity and has an additional overhead compared to a constantly powered rotor. However, our results will show that the power savings from duty-cycling substantially extend the blimp's lifetime.

3.2 Energy Harvesting

As it has been previously discussed, blimps have relatively low energy requirements for hovering. Thanks to our proposed power management techniques, these requirements can be reduced even further. Still, energy harvesting is necessary to allow for long-term autonomous operation.

Energy harvesting encompasses a variety of methods to acquire energy from the environment. Solar panels are most common, due to their high power densities and general availability of light. The power produced from a solar panel depends directly on the amount of light and size of the panel. The first parameter is environmental and cannot usually be controlled. The second parameter is an important design choice. Larger panels can naturally produce more power for a given amount of light, but there is a strict limit since every nano-UAV has a very tight payload. Due to the inherent variability of the energy input, there is a trade-off between the amount of energy a solar panel can harvest and its size/weight.

[1]Note that, a platform slightly lighter-than-air, coupled with a propeller generating lowering would be feasible as well. However, with this design the deflation of the balloon over time would require a second rotor generating lift.

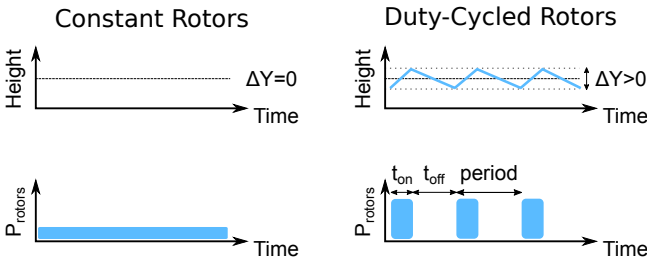

Figure 3: Duty-Cycling the rotors, when possible, brings significant energy savings at the expense of a larger Δ Y tolerance.

In energy-harvesting UAV's, where flight times depend on the amount of harvested energy, one of the most relevant parameters is *excess time* [5]. It measures how long the vehicle is able to fly without any energy input, or simply its minimum guaranteed flight time. This time is provided by batteries, and needs be chosen at design time. The total payload will then depend on the battery to solar panel weight ratio, which can be optimized for a given environmental setting. The payload optimization problem will be studied in greater detail in Sec. 4.2.

4 SYSTEM MODEL

In this section we introduce the models and methods for the system's analysis. The first model is used to understand the blimp's power requirements and to estimate the lifetime as a function of environmental conditions. The second model is used to explore the weight distribution problem in order to identify the best trade-off, between dimensions of the battery and the solar panel, for the desired lifetime.

4.1 Sustainability Model

In order to understand how power is harvested and consumed, and to estimate the lifetime of a given blimp, a sustainability model has been created. More precisely, the model we built takes the blimp's configuration and environmental conditions as input, and produces the expected flight time of the craft, where an infinite flight time means the system is self sustainable. By the blimp's configuration, we mean a given solar panel, battery, and a rotor. The rotor's configuration, intensity, power consumption, and the period when duty cycling is used, are included in the configuration as well. To imitate the inherently variable environmental conditions, we describe the harvested energy with a random variable. This implies that the flight time is modeled as a random variable as well.

With this in mind, we have created a discrete time Markov model. Generally speaking, Markov models use *states* to represent possible conditions the system could be in, while *transitions* between states are non-deterministic and happen with a certain probability. This means that, at a given time, the probability of the system being in each of the possible states is known.

In our model, the system's state corresponds to energy in the battery available for use. The probability of transitioning from one state to another is derived from the consumed and harvested energy the following way. We first subtract the energy consumed in a period, and then we add the energy harvested in the period. As the battery is finite in size, there are corner cases when the battery

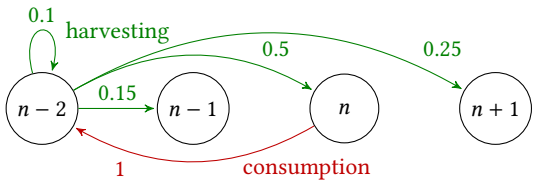

Figure 4: A transition from n to possible new states

is empty and full, and these will be discussed below. The time step of this discrete model is one duty-cycle period. There is a computational trade-off between the number of states and the accuracy of the model. However, we found a satisfactory solution by having the difference between two consecutive energy states an order of magnitude smaller than the energies consumed or harvested in one period.

Besides the many states representing different energy levels, there is an additional *error* state. This state is entered when the rotor fails to run due to insufficient energy. This state is absorbing, meaning that once entered, the system stays in the error state. Because we assume that energy is first consumed during a transition between two states, before being harvested, the whole analysis is pessimistic w.r.t. the error state. By observing the probability of the system being in the error state after running for an amount of time, we can understand whether the blimp is operating at that time or not.

The state representing the battery fully charged is also notable. This is because the battery is finite, and if too much energy is harvested, the battery saturates to the fully charged state.

Before formally defining the Markov model, we will present an illustrative example to familiarize the reader to the underlaying concepts.

Example. The example in Figure 4 helps to understand the system model. Let the system be in state n at time step τ, meaning its energy level is n at that time. We will determine the state of the system at the next time step $\tau + 1$, after one period of operation.

During the period, we assume energy is first consumed and then harvested. Assume that the difference between two energy levels is one energy unit. Let the system consume 2 units of energy per period, and harvest some units of energy per period with the following probabilities: $\left(\begin{smallmatrix}0 & 1 & 2 & 3\\ 0.1 & 0.15 & 0.5 & 0.25\end{smallmatrix}\right)$. In Figure 4, the two operations that make up one transition are marked red (consumption) and green (harvesting). We see that the system moves to one of these several states after the period: $\left(\begin{smallmatrix}n-2 & n-1 & n & n+1\\ 0.1 & 0.15 & 0.5 & 0.25\end{smallmatrix}\right)$. By continuing this analysis and having more transitions, the possible states the system is in after an arbitrary number of periods can be obtained. Please note that we have not depicted the corner cases in the example: the error state, which is entered when there is not enough energy to supply the rotor; and the full battery state, after which no more energy can be harvested. □

Formally, we define the state vector as (1), where $b_i^{(\tau)}$ is the probability that the system is in state i at time step τ, and $\sum_i b_i^{(\tau)} = 1$. There are N states representing different energy levels in the battery, and one error state.

$$b^{(\tau)} = \left(b_1^{(\tau)} \; b_2^{(\tau)} \; \dots \; b_N^{(\tau)} \; b_{\text{err}}^{(\tau)} \right) \tag{1}$$

We define the transition matrix T as a matrix whose element T_{ij} is the probability that the system transitions from state i to state j in one time step. As the time step of the model is one period, and we assume the consumption of energy happens first, we can write the transition matrix as $T = T_{\text{consume}} \times T_{\text{harvest}}$. Here T_{consume} represents removing energy from the battery, the amount depending on the energy consumed in a burst; while T_{harvest} represents adding energy to the battery, the amount likewise depending on the energy harvested in one period.

Combining all of the above, we can write the state of the system at time step τ as (2). Note that (τ) in the superscript notes a state vector corresponding to time τ, while τ in the superscript denotes the exponential.

$$b^{(\tau)} = b^{(\text{initial})} \times (T_{\text{consume}} \times T_{\text{harvest}})^{\tau} \tag{2}$$

Finally, we can define the system's lifetime as (3). We see that the system's lifetime is τ if, for some defined ϵ, the condition is met. If this condition is never met, we say that the system is self sustainable.

$$\text{lifetime is } \tau \quad \Leftrightarrow \quad b_{\text{err}}^{(\tau)} \leq \epsilon \wedge b_{\text{err}}^{(\tau+1)} > \epsilon \tag{3}$$

With the overall structure of the model in place, we can go into more detail regarding the period, battery, and the consumption and harvesting of energy.

Period. When the rotor operates with duty cycling, the period is the time between two consecutive bursts. Other behavior, the rotor running constantly and the harvesting of energy, is done constantly. To model these as periodic tasks, we take the period of the duty cycle, and assume that energy in added or removed once per period.

Battery State. The battery is not a perfect power supply. As the battery voltage level decreases below a certain point, the drone is unable to draw the amount of power required for the rotor. Experimentally, we observed that this level depends on the rotor configuration. The minimum voltage level is lower for constantly powered rotors than it is for duty cycling. We model the battery as a perfect power supply, but its capacity is adjusted such that it reflects the amount of usable energy it can provide to the rotor.

Blimp Power Consumption. The discharge rate depends on the way the rotor is configured to operate. When configured to constantly power the rotors, the energy consumption per period will be called E_{const}. Eq. (4) shows this energy to be simply the system's constant power consumption times the period.

$$E_{const} = P_{const} \cdot Period \tag{4}$$

When duty-cycling, the energy consumption per period, called E_{duty}, has several parameters. Eq. (5) shows it depends on the power consumption during the *on* and *off* periods (P_{on} and P_{off} respectively) and their duration (T_{on} and T_{off} respectively). Note that $T_{on} + T_{off} = Period$. There is one additional term, $E_{startup}$, which represents the overhead to turn on the motor in every period. This was omitted in the constant configuration, since it is incurred only once during the blimps entire lifetime.

$$E_{DC} = P_{on} \cdot T_{on} + P_{off} \cdot T_{off} + E_{startup} \tag{5}$$

As was mentioned in Sec. 3.1, the intensity of the rotor in duty-cycle mode is higher than in continuous mode, thus $P_{on} > P_{const}$.

Nonetheless, we have experimentally determined (see 6.1) that $E_{const} \approx 3 \cdot E_{DC}$. The energy consumption in each period is assumed to be constant. This means that each period, the battery state will decrease for a constant amount. For battery states that do not have sufficient energy for consumption, the system transitions to the error state.

Probabilistic Energy Harvesting. By probabilistic energy harvesting, we mean having the probability of adding an amount of energy to the battery during each time period. Note that the probability distribution of energy can vary depending on the environment, and we can analyze arbitrary probability distributions. This is especially useful for modeling harvesting based on measured data.

4.2 Dimensioning an Energy Harvesting Blimp

Every aerial vehicle has a limited payload it can lift. To maximize a blimp's lifetime requires solving a weight distribution problem, where the payload must be optimized to minimize the weight for both solar panel and battery. Thus, a well configured system should be able to harvest and store enough energy for the desired lifetime, saving as much weight as possible. Fundamental parameters to take into account are the target lifetime (τ) and the illuminance (intensity, variance and duration). Naturally, such parameters depend on the application scenario we want to address, and can vary significantly from one environment to another (e.g. indoor vs. outdoor).

The total weight of the system (W_{tot}) is then equal to the sum of each piece: the core frame (W_{frame}), the battery (W_{bat}), and the solar panel (W_{panel}). This total should be less than the maximum payload (W_{max}). The average power consumption of the vehicle (P_{load}) is supplied from both battery and solar panel. The input energy harvested from the solar panel (E_{in}) depends on the panel's area (that is proportional to its weight W_{panel}) and on the illuminance conditions ($Light$). The energy supplied by the battery (E_{bat}) depends on its weight W_{bat}. Thus we want maximize the lifetime τ, and respect the following conditions:

$$\begin{aligned} \tau \cdot P_{load} &\leq E_{in}(W_{panel}, Light) + E_{batt}(W_{batt}) \\ W_{tot} &\leq W_{max} \end{aligned} \tag{6}$$

Our proposed solution, to be discussed in detail in Sec. 6.1, will evaluate different weight distributions, and estimate the blimp's lifetime for both optimistic and pessimistic lighting conditions.

5 SYSTEM IMPLEMENTATION

The blimp prototype consists of three main components: the balloon, the rotorcraft, and the solar panel. Each of these components were carefully selected to optimize the flight time of the craft and will described in the next Sec. 5.1. Then, in Sec. 5.2, we will describe the software implementation of our power management.

5.1 Rotor Craft Setup

The solar panel is mounted to the top of the balloon and the rotorcraft is suspended from the balloon's underside. This setup can be seen in Fig. 5. The suspended rotorcraft requires a stiff harness to avoid swinging during flight and acting as a pendulum.

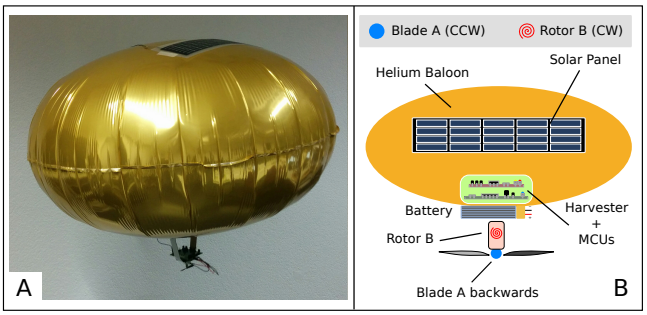

Figure 5: A: The blimp prototype during flight. B: The blimp model with solar panel, MCU's, battery, and rotor.

The rotorcraft is built using a modified, open-source/open-hardware nano quadcopter, the *Crazyflie 2.0*[2]. The quadcopter originally weighed 26 g including battery and flies for approximately 15 minutes per charge, in standard conditions. This craft was chosen due to the form factor and the open source design allowing flexible software and hardware modifications.

The main hardware of the drone is built around two MCU's, a collection of sensors, and four motors providing the lift. The frame of the craft is the circuit board itself and the motors attach to the PCB using plastic motor mounts. The radio communication and power management for the system is controlled using a *NRF51 MCU*[3]. The motors are controlled by an *ST STM32F405 MCU*[4] by pulse-width modulation (PWM) signals.

The craft was modified to provide lift to support the goal of hovering. Fig. 5-A shows the final design of the prototype. Only one motor is attached to the craft and is pointed downward to provide upward lift to the balloon. The single rotor was mounted in the center of mass, otherwise an oscillating movement would have been generated, compromising the stability of the system. The blade also had to be adjusted in order to have the desired thrust in the downward direction. This can be achieved combining the clockwise (CW) rotor with counter clockwise (CCW) airfoil mounted backwards, as depicted in Fig.5-B. The system is extended with the tiny *TI bq2920*[5] power charger to convert the energy harvested from the solar panel. Finally, all the hardware components are attached to the underside of the balloon using a lightweight frame.

The helium balloon used for the blimp is a commercially available, round mylar balloon with a 91 cm diameter. Mylar balloons are sturdier than the common latex balloon and have a lower gas permeability. This low permeability allows the balloon to stay inflated for longer than a latex balloon. Fig. 6 shows an empirical estimation of our balloon's deflation rate, starting with a fully inflated balloon over a period of 40 days. The balloon looses on average 0.35 g of lift per day, so even if a blimp has battery lifetimes of a few hundred hours, the helium lift can be assumed to be constant.

Experimentally we know the maximum lift of the balloon is about 55 g. All of the wires, battery, motor, solar panel, and hardware needs to fit under that weight budget. Our modified rotorcraft weights 11 g and the additional connections accounts for 4 g, thus

[2] http://www.bitcraze.io/crazyflie-2
[3] http://www.nordicsemi.com/Products/nRF51-Series-SoC
[4] http://www.st.com/en/microcontrollers/stm32f405-415
[5] http://www.ti.com/lit/gpn/bq29200

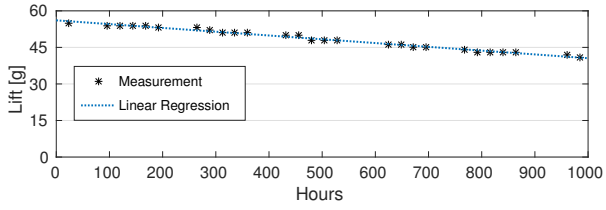

Figure 6: Lift decrease over 1000 hours due to helium leakage from the balloon.

the available payload left for both battery and solar panel is 40 g. In Sec. 6.1 we will evaluate the change in lifetime under different light conditions and battery/solar panel weights.

5.2 Power Management in Software

In the original firmware the NRF51 is designated as the main processor. It controls the radio communication between the drone and the base station, and it controls the power supply to the sensors and the STM32 MCU. The developers system diagram [25] for the original drone can be seen in Fig. 7.

At the system start-up the NRF51 turns on the STM32 MCU, enabling its power-domain. The STM32 firmware is based on a real time operating system. The operating system has a number of tasks that govern sensor reading, motor control, and communication between the two MCU's.

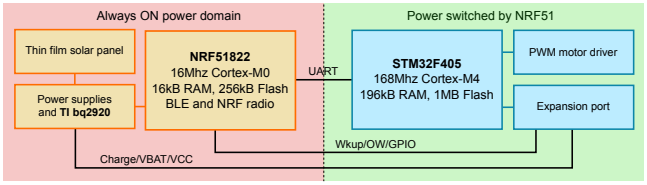

Figure 7: Crazyflie2.0 electronics diagram.

During normal operation the NRF51 consumes about 20 mW of power without the radio communication, and the STM32 and sensors consume about 180 mW of power. To enable power cycling to conserve power during flight, our firmware version keeps only the functionality strictly required for our goal.

The proposed simplified, low-power firmware is presented in Fig. 8. We kept the basic structure of the original firmware and we removed both the real-time operating system and the radio communication. The NRF51 and STM32 still govern the power distribution and the motor speed, respectively. The duty-cycling is enabled introducing in the NRF51 firmware a state machine that sets the *on* and *off* mode of the STM32. A timer in the same firmware is set to the desired duty cycle frequency and a master boot flag is set inside the interrupt, that is triggered by the timer. This boot flag controls the state machine. During the *on* phase it starts the STM32 and during the *off* phase it turns the STM32 off and drives the NRF51 to sleep mode to conserve power.

The sleep portion of the code is critical to reducing the consumed power of the system. The power consumed during the *off* state is $\sim 5\mu W$ and the power consumed during the *on* state is $\sim 4\,W$ when the rotor is set to full intensity.

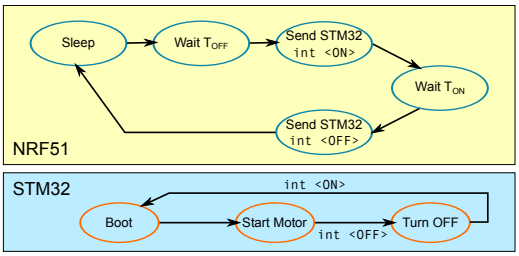

Figure 8: State diagram of the NRF51 and STM32 MCU's. The 'int <X>' labels indicate an interrupt for event X.

As introduced in Sec. 3, both duty-cycle and continuous mode operate with a static, predefined rotor intensity. The continuous mode can be enabled simply disabling the timer interrupt in the NRF51 firmware and boot the system directly to the STM32.

6 SYSTEM EVALUATION

In this section we provide all the experiments for a detailed comparison of our prototype with the Markov model presented in Sec. 4. For the sake of simplicity, our experimental results will be measured using one ratio and constant harvesting conditions. These will then be used to verify our model's predictions.

6.1 Initial Characterizations

To get a better understanding of the basic parameters of a hovering blimp, and to be able to use them as input for our models, we have performed a set of initial tests to characterize our blimp implementation.

Rotor Initialization Overhead. All electric motors, including our blimp's brushless motor, have a power curve that peaks initially and then settles. This incurs an activation overhead that was discussed in Sec. 4.1. Fig. 9 shows the power consumption of a single rotor running at 100% intensity for 2 seconds. It peaks to 5.75 W and 220 ms later, reaches a ~4.1 W steady state. From our initial experiment, we characterized this overhead as ~1.65 W for ~220 ms with a total energy of ~0.18 J.

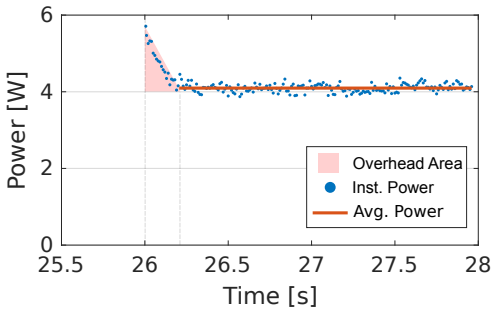

Figure 9: Power consumption of single rotor over two seconds @ 100% thrust.

Rotor Intensity and Duty-Cycle Selection. Our baseline hovering technique uses constant thrust to compensate for gravity, thus

maintaining the blimp at a constant altitude in a controlled environment. As was discussed in Sec. 3, the blimp requires relatively little rotor intensity to achieve this, thanks the lift provided by the helium. From our experiments, it was determined that only 9% rotor intensity was required for hovering. This results in a power consumption P_{const} =0.576 W.

To determine the optimal duty cycle we conducted flight tests and measured the blimp's vertical displacement for different duty cycles. We have set our maximum height deviation, called ΔY, to be $\pm 25\,cm$. Based on the collected data in Fig. 10, we can see that one *on* period (i.e. T_{on}) of 250 *ms* will cause the blimp to rise 50 *cm*. This displacement takes longer than 250 *ms* due to the balloon's inertia. The *off* period (i.e. T_{off}) needs to be long enough to allow the balloon to reach its maximum height and return to its initial position. This was experimentally determined to be 5 *s*. The selected duty-cycle of $T_{on} = 250\,ms$ and $T_{off} = 5\,s$, has an average power consumption P_{DC} =0.198 W (including the initialization overhead) and consumes 1.14 J, as shown by the orange line in Fig. 10. Though our duty cycle T_{on} is within the motor's current peak, our average power consumption is still be smaller P_{const}, thanks to the 5 *s* T_{off}.

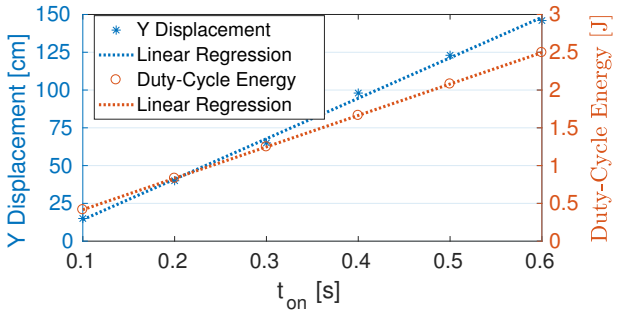

Figure 10: Measured vertical displacement (Y) and energy per period in duty-cycled blimp.

Optimized Weight Distribution. In order to analyze the weight distribution, we evaluate different batteries and solar panels sizes w.r.t. the available payload. As stated in Sec. 5, the payload of our blimp is of 55 *g*, but the actual weight budget we can spend for solar panel and battery is 40 *g*, due to the 15 *g* used for the rotorcraft and connections. The evaluated weight combinations are reported on the x-axis, with a growing step of 5 *g*. The blimp's lifetime in duty-cycling mode was calculated for each weight distribution under two different environmental conditions: a constant insolation of 39 *kLux* and 19.5 *kLux*.

In Fig. 11-A we can see how, even with favorable lighting conditions, the blimp's lifetime first decreases from configuration 0/40 to the 20/20 before increasing from configuration 25/15 to 40/0. The peak, with an infinite lifetime, is reached with the 40/0 configuration that represents the scenario where we use all the available payload for the solar panel. Although, this last case does not represent a feasible option in a real scenario due to the absence of any battery. The counterpart is represented by having only a 40 *g* battery without any solar panel and in this case the lifetime is 25 hours. In Fig. 11-B, we can see how the limited insolation makes the solar panel unable to extend the blimp's lifetime. In fact, even using the overall payload only for the solar panel, we would obtain a lifetime of 5 hours.

From the previous payload distribution results, it was determined that our nano blimp's payload should be distributed in the following way: 6 g for the battery, and 31 g for the solar panel. This distribution coincides with commercially available products and ensures that the blimp can, under optimistic conditions, fly for possibly over a hundred hours. At the same time, the blimp will have a minimum guaranteed flight time of several hours in pessimistic conditions.

6.2 Sustainability Model

The sustainability model, described in Section 4.1, was used to evaluate our prototype in order to estimate its lifetime. The model's estimates presented here are used to complement the experimental measurements.

Setup. The blimp's configuration, meaning the battery and the energy consumption, were based on the prototype. Two rotor's configurations were used, as introduced in the above sections. These are when the rotor is running constantly, and when it is duty cycled with a 0.25 second on and 5 second off time. For the environmental conditions, two hypothetical scenarios were used: when the harvested energy is constant, and when the harvested energy follows a probability distribution.

The Battery. It is, for the scope of the model, regarded as an ideal storage for energy. In reality the battery is not ideal, and we have observed, in Sec. 6.1, that only a certain amount of energy can be drawn from a fully charged battery. The measurements show that the amount of energy that can be drawn depends on the rotor's configuration. We believe this difference to arise from the power peak necessary to turn on the rotors in the duty-cycling configuration. This requires a higher battery voltage and thus reduced the amount of available energy.

We thus have two ideal batteries in the model, the constant configuration battery and the duty cycle configuration battery, and we use one depending on the rotor's configuration. The capacities of these two batteries were empirically obtained in the above mentioned measurements, and are 3156 Joules and 2767 Joules respectively. We assume in the model that the battery is always initially charged.

The Consumed Energy. It depends on the rotor's mode of operation as well. Experiments determining the rotor's consumption were done in Section 6.1. Our sustainability model is a discrete time model where the time step is the duty cycling period, 5.25 seconds. When the rotors run constantly, they consume 0.576 *W*. Thus, the energy per period is E_{const}=3.024 J. Likewise, for duty cycling, we measured that the rotor consumes an average of 4.16 *W*. This results in an energy per period of E_{DC}=1.04 *J*.

Harvested Energy. It depends on the environmental conditions, and two hypothetical scenarios were used in the model. The first one was when the amount of energy harvested was the same each time step. This constant scenario is fairly simple, and is an obvious choice for comparison with other results. The second environmental scenario used was when harvested energy follows a logarithmic-normal distribution with a standard deviation of $\sigma = 0.5$. The log-normal distribution is the logarithm of a normal distribution. It was chosen for the scenario as a first approximation of variable

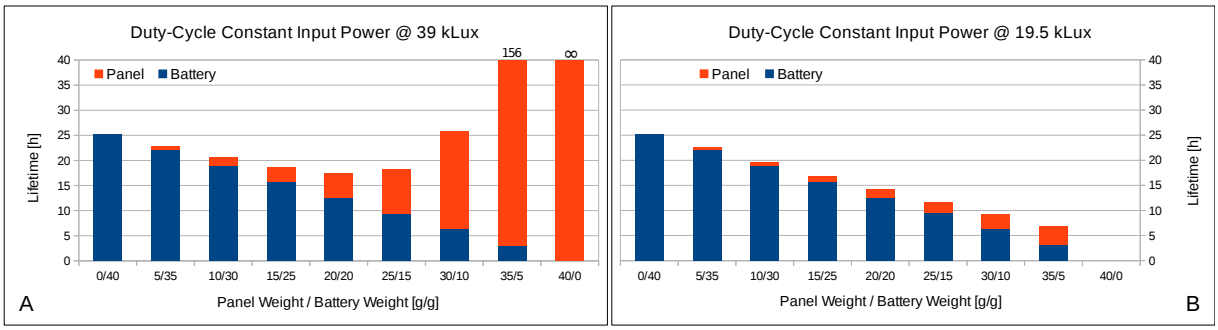

Figure 11: Weight distribution evaluation for constant input power. A - @ 39 $kLux$ and B - @ 19.5 $kLux$

environment conditions. An example of a log-normal distribution used, with the mean value at 0.1 W and 0.5 standard deviation, is shown in Figure 12a.

Results. Using the sustainability model, we evaluated the two rotor modes of operation in two hypothetical environmental scenarios.

Constant Energy Harvesting. The blimp's estimated lifetime, when the input energy was constant every time step, can be seen in Fig. 13. The lifetime when the rotor runs constantly is marked as 'Const. Model', and 'D.C. Model' is used to label duty cycling. Note that the figure uses input power as the x-axis, so use that the period is 5.25 seconds to convert the power values to energy.

It should be noted that there is a vertical asymptote at $x = 0.198$ W, which is the point at which self sustainability is reached for D.C. hovering. Due to the increased power requirements of Const. hovering, this configuration's asymptote is located at $x = 0.576$ W.

Probabilistic Energy Harvesting. To next scenario used was one that approximates volatile lighting conditions, where the energy harvested follows a probabilistic distribution.

Before going into the results, we first need to comment on the definition of the lifetime, presented in (3). As stated in Section 4.1, the sustainability model provides us with the probability of the system being in a certain state after some time. Therefore, we need to define a threshold ϵ, such that the system is defined not to work if the probability of the system being in the error state is larger than ϵ. As (3) shows, the lifetime is a function of the ϵ, so we estimated the lifetime using $\epsilon = 10^{-4}$. A lifetime with $\epsilon = 10^{-4}$ means that 999 blimps out of a 1000 are estimated to be working after this time. We shall call this ϵ choice the pessimistic case.

The pessimistic case's lifetime estimation is influenced by periods that harvest low amounts of energy, even though these cases happen less often. In Figure 12b, the relative difference between the average and pessimistic lifetimes is shown. Recall that the absolute values for these lifetimes can be seen in Fig. 13. What can be seen is that the pessimistic lifetime is estimated to be around 5% shorter than the lifetime when energy is added constantly, and this difference increases as the lifetime rises.

6.3 Experimental Measurements

Using the prototype's specification explained in Section 6.1, we evaluated our proposed power management techniques for nano blimps. To this end, we use two configurations, one with constant propulsion hovering (referred to as 'Const.') and another with duty cycling (referred to as 'D.C.'). For each configuration, we determined how different input power levels affect the blimp's lifetime.

Setup. Experiments with different input powers were set up for both configurations. The battery was initially charged for each experiment, and the blimp's lifetime was recorded. The lifetime is defined as the point at which the rotors stop producing enough lift to keep the blimp within the desired ± 25 cm altitude window.

It should be noted that although the rotors continued to generate some lift after that, the battery was unable to supply the necessary

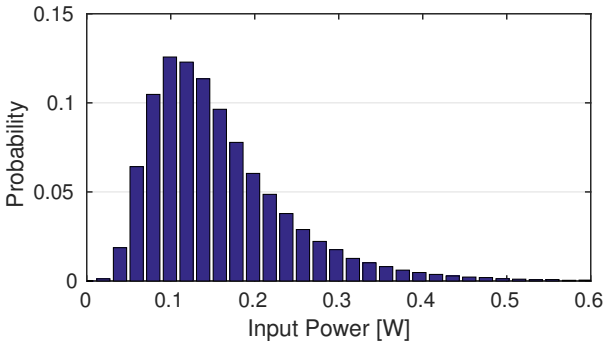

(a) Harvested power distribution used in scenario

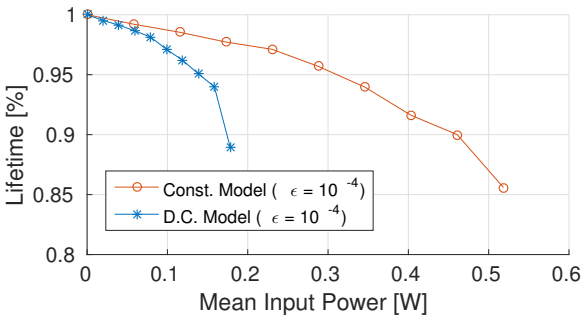

(b) Lifetimes for probabilistic harvesting, relative to constant harvesting

Figure 12: Normalized lifetime results using the sustainability model and a scenario with variable input power

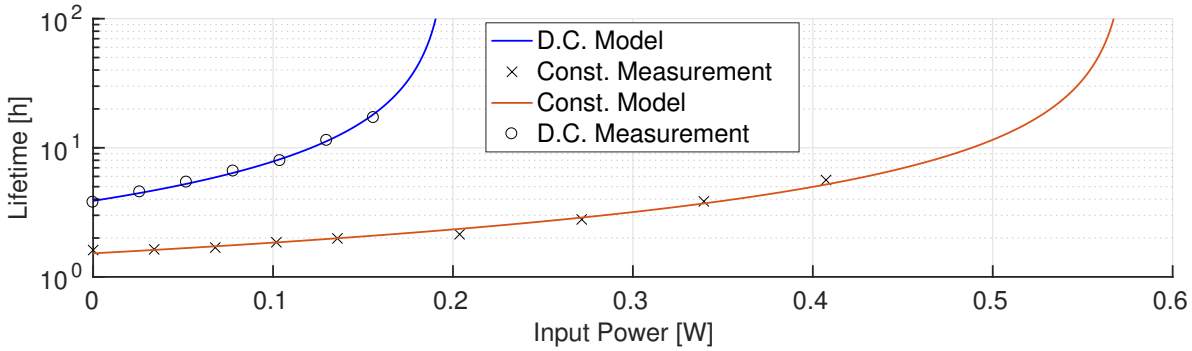

Figure 13: Measured lifetimes as a function of constant input power.

power to maintain the blimp within the desired tolerance. This behavior was not considered correct and did not contribute to the lifetime.

Results. Fig. 13 shows the results of the experiments for both configurations. The logarithmic y axis shows the system lifetime, while the x axis is the (constant) input power the system was configured to have. The two lines in the plot represent the sustainability model results, described in Sec. 6.2. The marked points from each line indicate measurements made using the nano blimp prototype. The extended lifetimes of D.C. hovering clearly demonstrate the impact of the proposed power management. As well as this, we can see that measurements follow the model's predictions. As was mentioned in Sec 3.2, the *excess time* is the system's lifetime without any input power ($x = 0$ mW). For the D.C. hovering configuration, the excess time is 3.78 hours, which is around 135 % longer than the Const. hovering configuration.

7 CONCLUSIONS

As nano UAV's have become more ubiquitous in recent years, many application domains would greatly benefit from extended flight times. We have presented a nano blimp platform which is inherently safe thanks to its helium balloon and uses duty-cycling to reduce its average power consumption for hovering. Using a sustainability model based on Markov chain analysis, we have analyzed the different input power conditions necessary to achieve self-sustainability with energy harvesting. The nano blimp's payload of 55 g has been optimized to include both a battery and a solar panel, which enables it to extend its lifetime to 100's of hours under normal lighting conditions. Extensive experimental results have demonstrated the validity of our model and power management. These steps form a solid groundwork for future autonomous nano UAV's which are safe and have extended flight times.

ACKNOWLEDGMENTS

This work has been funded by projects EC H2020 HERCULES (688860), Nano-Tera.ch YINS, and Transient Computing Systems (SNF grant 157048). The authors thank Lukas Sigrist for his support.

REFERENCES

[1] J. Kim *et al.*, "On the scheduling of systems of uavs and fuel service stations for long-term mission fulfillment," *Journal of Intelligent & Robotic Systems*, pp. 1–13, 2013.
[2] X. Zhang *et al.*, "Autonomous flight control of a nano quadrotor helicopter in a gps-denied environment using on-board vision," *IEEE Transactions on Industrial Electronics*, vol. 62, no. 10, pp. 6392–6403, 2015.
[3] A. Briod *et al.*, "Optic-flow based control of a 46g quadrotor," in *Workshop on Vision-based Closed-Loop Control and Navigation of Micro Helicopters in GPS-denied Environments, IROS 2013*, no. EPFL-CONF-189879, 2013.
[4] D. Palossi *et al.*, "An energy-efficient parallel algorithm for real-time near-optimal uav path planning," in *Proceedings of the ACM International Conference on Computing Frontiers*, ser. CF '16. New York, NY, USA: ACM, 2016, pp. 392–397. [Online]. Available: http://doi.acm.org/10.1145/2903150.2911712
[5] S. Leutenegger *et al.*, "Solar airplane conceptual design and performance estimation," in *In Proceedings of the 3rd International Symposium on Unmanned Aerial Vehicles*, 2010.
[6] M. C. Achtelik *et al.*, "Design of a flexible high performance quadcopter platform breaking the mav endurance record with laser power beaming," in *Intelligent robots and systems (iros), 2011 ieee/rsj international conference on.* IEEE, 2011, pp. 5166–5172.
[7] N. A. Bhatti *et al.*, "Energy harvesting and wireless transfer in sensor network applications: Concepts and experiences," *ACM Transactions on Sensor Networks (TOSN)*, vol. 12, no. 3, p. 24, 2016.
[8] M. Burri *et al.*, "Design and control of a spherical omnidirectional blimp," in *2013 IEEE/RSJ International Conference on Intelligent Robots and Systems*, Nov 2013, pp. 1873–1879.
[9] P. Li *et al.*, "Monocular snapshot-based sensing and control of hover, takeoff, and landing for a low-cost quadrotor," *Journal of Field Robotics*, vol. 32, no. 7, 2015.
[10] D. Falanga *et al.*, "Aggressive quadrotor flight through narrow gaps with onboard sensing and computing," *arXiv preprint arXiv:1612.00291*, 2016.
[11] R. Wood *et al.*, "Progress on 'pico' air vehicles," *Int. J. Rob. Res.*, vol. 31, no. 11, 2012.
[12] B. Siciliano and O. Khatib, *Springer handbook of robotics.* Springer, 2016.
[13] P. Oettershagen *et al.*, "A solar-powered hand-launchable uav for low-altitude multi-day continuous flight," in *Robotics and Automation (ICRA), 2015 IEEE International Conference on.* IEEE, 2015, pp. 3986–3993.
[14] S. Verling *et al.*, "Full attitude control of a vtol tailsitter uav," in *2016 IEEE International Conference on Robotics and Automation (ICRA)*, May 2016, pp. 3006–3012.
[15] R. Lozano, *Unmanned aerial vehicles: Embedded control.* John Wiley & Sons, 2013.
[16] M. H. Shaheed *et al.*, "Flying by the sun only: The solarcopter prototype," *Aerospace Science and Technology*, vol. 45, pp. 209–214, 2015.
[17] T. J. Nugent and J. T. Kare, "Laser power for uavs," *Laser Motive White Paper-Power Beaming for UAVs, NWEN*, 2010.
[18] S. Leutenegger, "Unmanned solar airplanes: Design and algorithms for efficient and robust autonomous operation," Ph.D. dissertation, ETH-Zürich, 2014.
[19] A. Weider *et al.*, "Sunsailor: solar powered uav," *Technion IIT, Haifa, Israel*, 2006.
[20] T. E. Noll *et al.*, "Investigation of the helios prototype aircraft mishap volume i mishap report," *Downloaded on*, vol. 9, p. 2004, 2004.
[21] J. Li *et al.*, "Optimum area of solar array for stratospheric solar-powered airship," *Proceedings of the Institution of Mechanical Engineers, Part G: Journal of Aerospace Engineering*, p. 0954410016670420, 2016.
[22] H. Liang *et al.*, "Conceptual design optimization of high altitude airship in concurrent subspace optimization," in *50th AIAA aerospace sciences meeting including the new horizons forum and aerospace exposition*, 2012, p. 1180.
[23] W. Knaupp and E. Mundschau, "Photovoltaic-hydrogen energy systems for stratospheric platforms," in *3rd World Conference onPhotovoltaic Energy Conversion, 2003. Proceedings of*, vol. 3, May 2003, pp. 2143–2147 Vol.3.
[24] K. Ghosh *et al.*, "Power generation on a solar photovoltaic modules integrated lighter-than-air platform at a low altitude," *arXiv preprint arXiv:1610.07598*, 2016.
[25] Bitcraze. (2016) System diagram.